Acta Scientiarum

http://www.uem.br/acta
ISSN printed: 1806-2563
ISSN on-line: 1807-8664
Doi: 10.4025/actascitechnol.v39i4.29032

Experimental investigation on streamlines in a 180º sharp bend

Maryam Akbari and Mohammad Vaghefi*

*Department of Civil Engineering, Persian Gulf University, ShahidMahini Street, P.O. Box: 75169-13817, Bushehr, Iran. *Author for correspondence. E-mail: vaghefi@pgu.ac.ir*

ABSTRACT. One of the most important concerns of hydraulics engineers is predicting erosion at the outer banks of rivers by studying the flow pattern along the bend. Not only are the streamlines in meanders non parallel curved lines, but they are also twisted. To study the streamlines flowing a sharp bend, a 180º sharp bend was constructed at Persian Gulf University in Iran. Three dimensional flow components at different locations of the bend were measured using Vectrino velocim. In this paper, streamlines were drawn and investigated in different longitudinal profiles, cross sections, and plans. The results indicated that the secondary flow strength and size of the vortex formed at the distance of the beginning to the bend apex would increase. The core of central vortex moved away from the inner bank towards central line of the channel by 22%, and to the water surface by 20%. On the contrary, the size of the secondary vortex increased by 15%. In addition, the average of the horizontal angle of the streamlines, vector and the locus of maximum velocity were determined at different levels in the present investigation.

Keywords: secondary flow, longitudinal pressure gradient, Vectrino, laboratory bend flume, flow velocity, cross pressure gradient.

Investigação experimental sobre linhas de fluxo numa curva acentuada de 180°

RESUMO. Uma das preocupações mais importantes de engenheiros de sistema hidráulico é prever a erosão das margens de rios estudando o padrão de fluxo ao longo da curva. Além das linhas de fluxo no meandro não serem paralelas, elas são torcidas. Para estudar as linhas de fluxo através de uma curva acentuada, uma curva de 180º foi construída na Universidade do Golfo Pérsico no Irã. Componentes do fluxo tridimensional em diferentes locais da curva foram medidos usando velocímetros de Vectrino. Neste artigo, as linhas de fluxo foram desenhadas e investigadas em diferentes perfis longitudinais, transversais, e planos. Os resultados indicaram que a força e o tamanho do fluxo secundário do vórtice, formado do início para o pico da curva tendem a aumentar. O núcleo central do vortex moveu-se, da margem para a linha central do canal em 22%, e a superfície da água em 20%. Ao contrário, o tamanho do vórtice secundário aumentou 15%. Além disso, a média do ângulo horizontal das linhas de fluxo, o seu vetor e o local da velocidade máxima foram também determinados em diferentes níveis no presente estudo.

Palavras-chave: fluxo secundário, gradiente de pressão longitudinal, Vectrino, canal curvo de laboratório, velocidade de fluxo, transversal gradiente de pressão.

Introduction

The secondary flow is formed as a result of centrifugal force and its interaction with lateral pressure gradients due to lateral slope of water surface. In this flow, water moves away at the upper part of the river, and at the lower part, it moves towards the inner bank. In open-channel bends, the curvature of the flow gives rise to secondary flow, resulting in the helical motion. This helical motion is of high importance in meandering rivers, where it plays a key role in erosion and sedimentation patterns in the river's bed (Van Balen, Uijttewaal, & Blanckaert, 2009). Therefore, it is vital to know about and study flow pattern in river bends in order to predict and prevent outer wall erosion in the rivers. Moreover, the proper understanding of flow characteristics in curved open-channels is vital in predicting the spreading of pollutants and thus for water quality of natural river systems (Van Balen et al., 2009).

Since scour and flow patterns are of high importance in river and hydraulics engineering, a great number of researchers have always conducted studies on flow structure and sediment transport through bend and straight reaches. Kra and Merkley (2004) developed a computational method based on mathematical modeling for both two-dimensional and three-dimensional velocity distributions for steady-state uniform flow in open channels of rectangular cross-section. It is evident that the two-dimensional version of the model is not appropriate

for calculating surface velocity coefficients. Sui, Fang, and Karney (2006) carried out an experimental study on local scour in a flume with a 90º bend and analyzed the effect of some param including the Froude number, slope and width of the protective wall, and size of bed particle on the scour at bed level. Huang, Jia, Hsun-Chuan, and Sam (2009) applied NCCHE3D 3-D free surface to study secondary flows in an experimental channel. The agreements of vertically-averaged velocities between the simulated results were obtained by using different turbulence models with different pressure solution techniques, and the resulting measured data were satisfactory. Wang, Zhou, and Shao (2010) used a computational fluid dynamics model for simulation of two-dimensional water flow, sediment transport, bank failure processes, and the subsequent channel pattern changes. They considered the effects of secondary currents in bend channel and validated the water flow model using experimental data. Experimental and numerical studies of flow pattern in a 90º bend by Abhari, Ghodsian, Vaghefi, and Panahpur (2010) indicated that streamlines at the level close to the bed orient to the inner wall and at levels near water surface decline to the outer wall. Chan, Zhang, Leu, and Chen (2010) studied the turbulent flow in a channel with periodic porous ribs on one wall. They used the Reynolds averaged Navier-Stokes (Rans) equations with a k-ε turbulent model for turbulence closure. Barbhuiya and Talukdar (2010) carried out an experimental study of three dimensional flow and scour pattern in a 90º bend, and measured the time averaged velocity components, turbulent intensity components and Reynolds stresses in different vertical sections by using ADV. The Results showed that the maximum measured velocity is 1.61 times the mean velocity. Stoesser, Ruether, and Olsen (2010) solved the Navier–Stokes equations on a fine three-dimensional grid by using a Large Eddy Simulation approach and a method that is based on the Rans equations for which there are two different isotropic turbulence closures. The results provided clear evidence that the Rans code was able to predict the time-averaged primary velocities with good agreement regardless of the turbulence model used. Bonakdari, Baghalian, Nazari, and Fazli (2011) predicted flow field in a mild 90º bend using Artificial Neural Networks (ANN) and Genetic Algorithm (GA). They studied the variations of velocities in both experimental and numerical (CFD) models. Moreover, they compared the results of ANN and CFX methods in sections where experimental data were not available. Constantinescu, Koken, and Zeng (2011) considered the flow in an open channel bend of strong curvature (the ratio between the radius of curvature of the curved reach and the channel width is close to 1.3) over realistic topography corresponding to equilibrium scour conditions. Results demonstrated that compared to Rans, DES (detached eddy simulation) is able to better capture the redistribution of the mean flow stream wise velocity. Baghalian, Bonakdari, Nazari, and Fazli (2012) investigated the velocity field in a 90 degree open channel bend using artificial intelligence, analytical, experimental, and numerical methods. They indicated that numerical, ANN and experimental results could show that the maximum velocity occurs under the free-surface but the analytical solution could not. Blanckaert et al. (2013) studied three distinct processes of flow separation near the banks in sharply-curved open-channel bends. The experiments were performed with both a flat immobile gravel bed and a mobile sand bed with dominant bed load sediment transport. Gholami, Akhtari, Minatour, Bonakdari, and Javadi (2014) carried out the experimental and numerical modelling of flow pattern at a strongly-curved 90 degree bend and reported that in both models, along the bend, the maximum velocity always occurs near the inner wall while the minimum occurs near the outer wall. Celik, Diplas, and Dancey (2014) measured the pressure fluctuations on the surface of a coarse, fully exposed, spherical grain resting upon a bed of identical grains in an open channel turbulent flow. They concluded that the stream wise velocity near the bed is most directly related to those force events crucial to particle entrainment. Huang, Li, Huang, and Liou (2014) acquired temperature profiles in a PDMS micro channel with a 90º sharp bend using a molecule-based temperature sensor. These temperature evolutions agree with secondary flow patterns identified from the velocity measurement. Vaghefi, Akbari, and Fiouz (2014) used the Depth-Averaged method to study and analyze shear stress distribution near the bed in a 180º sharp bend flume. The results suggested that the maximum dimensionless shear stress occurs near the inner wall and at the 40º cross section. Vaghefi, Akbari, and Fiouz (2015) measured three dimensional flow velocity components in a 180 degree sharp bend. The comparison between the longitudinal velocity values at distances of 5 and 95% from the bed showed a 60% increase in flow velocity from near the bed to water surface. Horvat, Isic, and Spasojevic (2015) applied a two-dimensional numerical model for simulating water flow, sediment transport and bed evolution in a straight channel. The simulation results showed

good agreement with the field measurements, and the continuity equation error was negligible for both water and sediment computation. Termini (2015) investigated the role of advective momentum transport by cross-circulation in bed shear stress distribution along a meandering bend. Based on the measured data, he proposed an equation expressing the relationship between cross-sectional momentum and downstream velocity. As observed, most of the investigations carried out on flow pattern in the past were done on a straight route or merely on scour pattern or shear stress calculations as far as experiments were concerned. Moreover, no experimental studies have been conducted on a 180 degree sharp bend with R/B = 2 (the ratio of central radius to channel width equals 2) to determine 3D flow pattern and streamlines so far. Due to development of secondary flow in a 180 degree bend and main factors of forming the flow through river bends including central angle of the bend and the ratio of curvature radius to channel width, this study has addressed streamlines' features in a 180 degree sharp bend (with R/B = 2). Thus, the flow velocity components have been recorded using Vectrino velocim in three directions, and the streamlines have been depicted and analyzed at longitudinal profiles, cross sections and plans. Moreover, the average of horizontal angle of the streamlines, vector, and locus of maximum velocity at different levels were subsequently determined and the results have been analyzed.

Material and methods

To carry out the experiment, a 1 m wide bend flume with a 180 degree central bend, which has glass walls supported by steel frames, was designed and constructed in the Hydraulic Laboratory of Persian Gulf University in Iran. The schematic view of the plan, cross section, and the geometric features of this flume are presented in Figure 1. As evident, the flume is composed of a 6.5 m long upstream and a 5.1 m long downstream straight reach, both connected via a 180 degree bend with an external curvature radius of 2.5 m and an internal curvature radius of 1.5 m (R/B = 2). Moreover, the flume depth is 0.7 m. The channel bed is assumed rigid and covered with uniform sediment with an average diam of 1 mm. Besides, the ratio of the mean flow velocity to the critical velocity (U Uc^{-1}) equals 0.98. Centrifugal pump's discharge capacity is 95 L s^{-1} which is supposed to be constant during experiments. The flow depth remains unchanged, equal to 20 cm at a one meters distance from the entrance of the bend, which is adjusted for the sake of the experiment by using the butterfly gate at the end of downstream reach. Accordingly, the Froude number and Reynolds number are equal to 0.34 and 67857, correspondingly. To measure 3D water velocity through this experiment, the Vectrino is used, which is considered a high-resolution Acoustic velocim. The Vectrino velocim measures flow velocity employing the Doppler Effect. This device consists of two different probes. The side looking probe is used to measure the flow velocity near walls of flume and the water surface, and the down looking probe is applied in other locations. The velocity values are in the range of ± 0.01 to ± 7 m s^{-1}, and this is adjustable for the user with ±5% measured accuracy (±1 mm s^{-1} – Vaghefi et al., 2014).

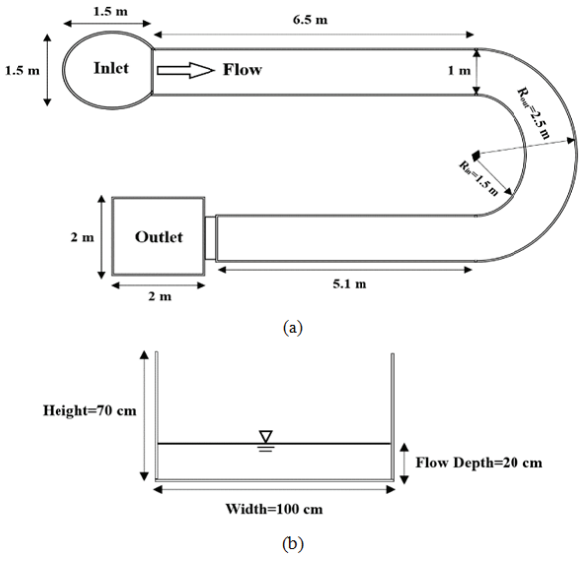

Figure 1. The schematic view of a) plan and b) cross section of the laboratory flume.

The experiments were carried out at a 25 Hz frequency in one minute. As such, the device can record up to 1500 data of the flow velocity per second in three directions. The collected data in various time series are recorded by Vectrino Software and transferred to Explorer V Software to process. Figure 2 demonstrates the location of the Vectrino velocim and its probes in the bend for recording 3D velocities values.

Twenty three sections from beginning to end of the bend, each of which has twelve cross sections, are used in order to measure flow velocity along the bend. As seen in Figure 3, a schematic view of meshing applied through the bend is presented in a plan and at a cross section that are essential to collect data.

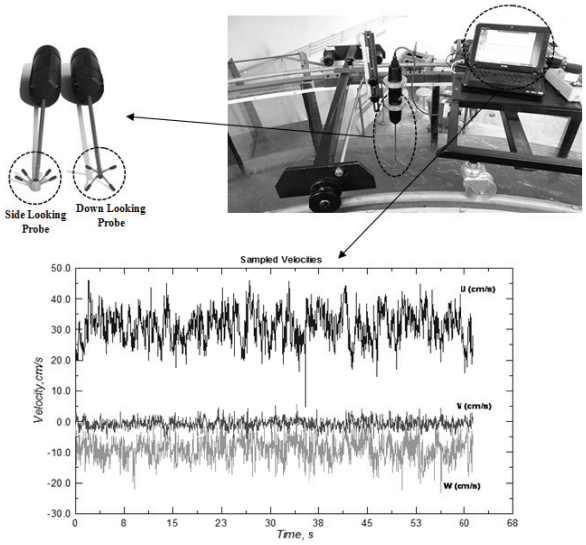

Figure 2. The location of Vectrino velocim and its probes in the bend for collecting and recording three dimensional velocities.

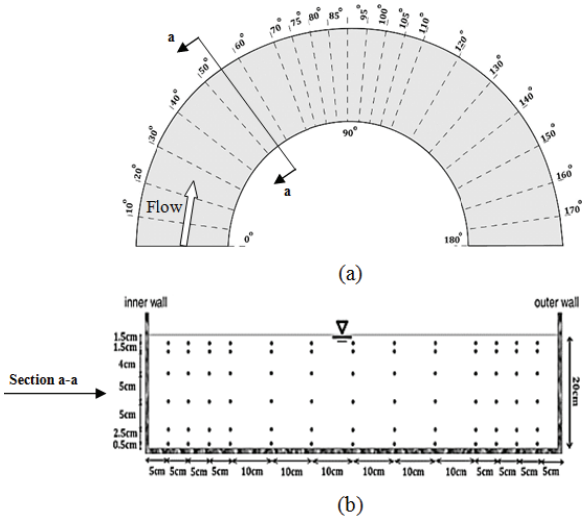

Figure 3. A schematic view of mesh used in the bend to collect velocities at various points, in a) plan and b) cross section.

Results and discussion

In this section, due to investigation of param affecting the mean flow pattern along 180° sharp bend, the streamlines variations at longitudinal profile, cross sections and plans have been analyzed. Then, the average of streamlines angles has been determined and eventually the location of the maximum velocity and its vector has been addressed.

Streamlines in cross sections

When flow enters the bend, drastic changes occur in its three dimensional velocity components due to existence of the secondary flow and longitudinal pressure gradient. For this reason, studying the streamlines in river bends is a matter of great importance. To investigate streamlines from the beginning to the end of the 180° sharp bend, they are shown at various cross sections (20, 60, 80, 90, 100, 120, 140, and 160°) in Figure 4. In the mentioned figures, B represents width of the channel, and Z the water level. In these cross sections, the longitudinal pressure gradient near the bed in the direction of the internal bend overcomes centrifugal force, and water near the bed is driven towards internal bend. On the other hand, that on the river surface is driven towards the external bend. As seen in Figure 4a, since the longitudinal pressure gradient dominates the secondary flow at the entrance of the bend, a primary and incomplete clockwise vortex is formed at the 20 degree cross section near the inner wall. As the secondary flow gains strength further on the route, the vortex evolves into a more complete form at the 60 degree angle (Figure 4b). Comparing the vortices in Figure 4a and b, it can be concluded that the location of this vortex moves away from the water surface towards the central line of the channel until it extends through channel width. Towards the apex of the bend, at 80 degree and 90 degree locations (Figures 4c and d), since the secondary flow reaches its highest strength, the clockwise vortex is fully formed at distances of 25 and 38% of channel width from inner bank and at levels of 60 and 65% of the flow depth from the bed, respectively.

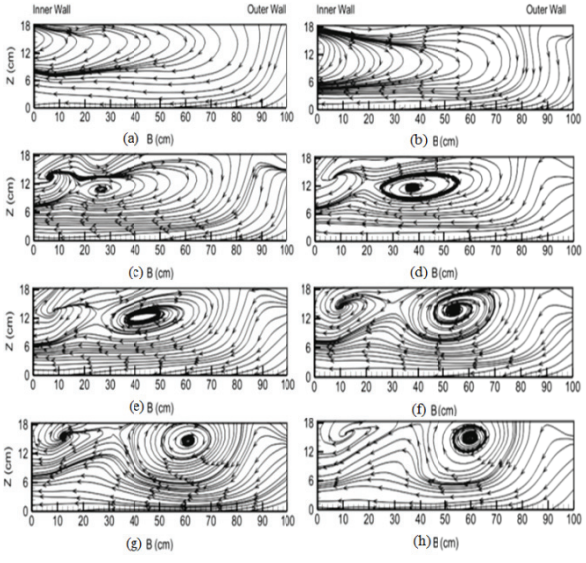

Figure 4. Streamlines through 180° sharp bend at: a) 20, b) 60, c) 80, d) 90, e) 100, f) 120, g) 140, and h) 160° cross sections.

As seen in these figures, there is another clockwise vortex in each section, called 'the secondary vortex', which is formed at a distance of

5% of channel width from the inner bank, at a level of 70% of the flow depth from bed. As the flow passes through the 90º cross section into the second half of the bend (Figures 4e to g), since the bend under investigation is 180º, the strength of the secondary flow decreases. Thus, the size of primary clockwise vortex in the center of the channel reduces while that of the secondary vortex rises. The secondary flow still exists near the end of bend, at 160ºcross section (Figure 4h), and a clockwise central vortex can be seen near the water surface, at a distance of 60% of the channel width from inner bank and level of 80% of the flow depth from bed. Moreover, the secondary vortex has become larger in comparison with that at the previous sections. Blanckaert and Graf (2001) had previously reported the second rotational cell at the 60 degree cross section near outer bank and stated that the vortex was directed against main vortex in a 120 degree sharp bend.

Generally, the changes observed in streamlines from the beginning of the second half of bend to the bend exit indicate that the core of central vortex has moved away from the inner bank towards the middle of channel by 22%, and towards the water surface by 20%. It can be deduced from figures in Figure 4 that there was a 15% increase in the size of the secondary vortex from the time it was formed until it reached the end of bend.

Streamlines through longitudinal profiles

In Figure 5, streamlines are shown in different longitudinal profiles at distances of 5, 15, 30, 50, 85, and 95% of the channel width from the outer bank. The streamlines are down flow from the bed up to a level of 80% of flow depth from the bed, but at higher layers, especially from the beginning of the second half of the bend to the end of it, streamlines are up flow (Figure 5a). Away from the external bend, flow turns into down flow in the longitudinal section at distances of 15 and 30% of the channel width from outer bank (Figures 5b and c). As displayed in Figure 5d, in the middle of channel width, the flow at a distance from near the bed up to 40% of flow depth from bed is in the same direction as the main flow, but thereafter, especially when it reaches the second half of the bend, it changes into up flow. The streamlines near inner bank are presented in Figures 5e and f, and it can be seen that from lower layers up to a level of 70 to 80% of the flow depth from bed, the flow is down flow. Afterwards, particularly from the beginning of the 75 degree cross section to the end of the bend, the flow is up flow due to formation of the secondary vortex near inner bank at cross sections (Figures 4c to h). The change from down flow into up flow in different longitudinal sections can be attributed to the vortices formed in different cross sections just before the beginning of the bend to bend exit, and furthermore, to the sharpness of the bend which drives the streamlines against walls.

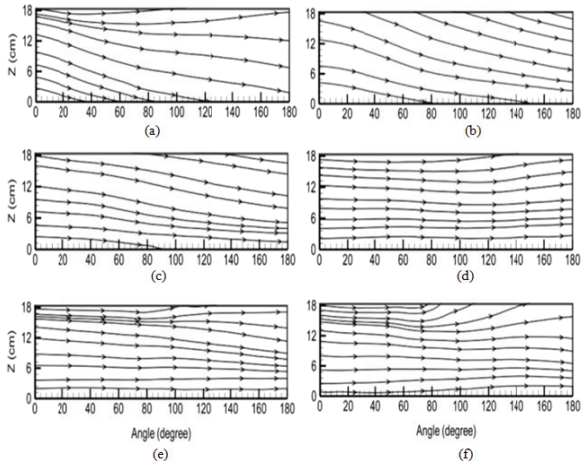

Figure 5. Streamlines in different longitudinal profiles in the 180 degree sharp bend at distances of a) 5, b) 15, c) 30, d) 50, e) 85, and f) 95% of the channel width from the outer bank.

Streamlines in plans

In Figure 6, the streamlines are shown in three different plans including near the bed, mid-depth, and near the surface (at levels of 5, 50, and 95% of the flow depth from bed of channel). In Figure 6a, it can be seen that the streamlines are oriented towards the inner wall from the beginning of the bend, and that thereafter, the flow is also rushing from the outer bend towards the inner bend. Such a phenomena is also observed in the second half of the bend until the streamlines at the end of bend move away from external bend towards mid-channel. The sharpness of 180 degree bend (with R/B = 2) causes the diversion in the streamlines. All mentioned features above are considered, and due to longitudinal pressure gradient's dominance, the streamlines extend towards inner; hence it can be concluded that scour at the inner wall of bend at the layer near the bed is highly probable to occur if the bed is moveable. Figure 6b depicts the streamlines being in the same direction as the curve of bend at mid-depth. This leads to change in direction of the streamlines near the bed as a result of formation of the vortices which were already described in Figure 4. However, from the beginning of the second half of bend, near inner wall, the streamlines strike at inner wall. As seen in Figure 6c, the streamlines near water surface are in the same direction as the curve of the bend, from the inner

wall to the mid-width of channel, and thereafter the flow is directed towards external bend. The change in orientation of the streamlines near surface in proportion to that near the bed is due to the secondary flow and longitudinal flow merging into each other and forming a spiral flow. Hence, where the bank is movable, erosion in the wall of the outer bank due to flow rush is highly probable. These results are consistent with those obtained from Leschziner and Rodi (1979) and Rozovskii's (1961) investigations.

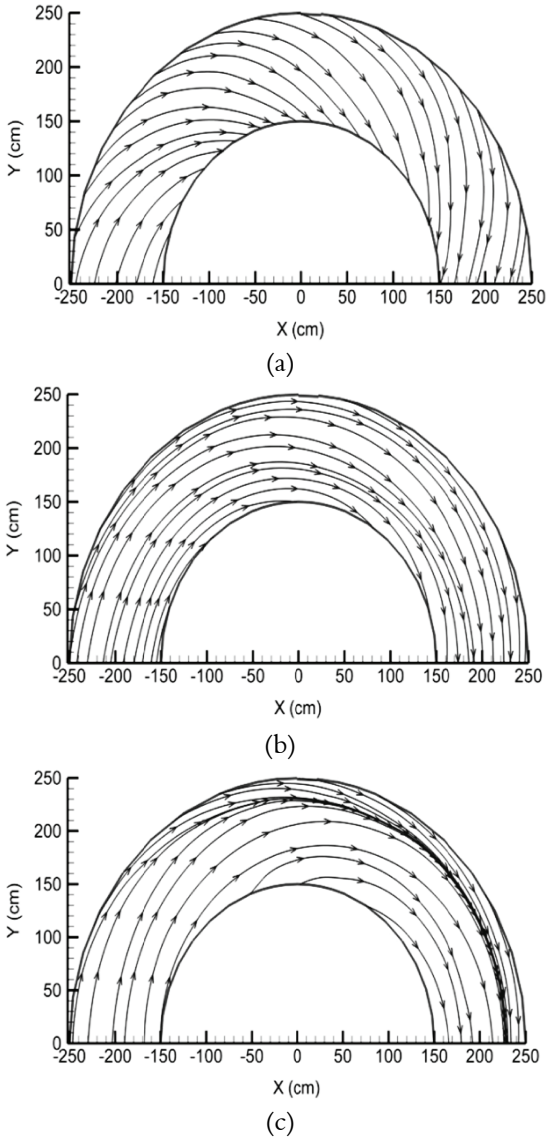

Figure 6. Streamlines in plans of 180 degree sharp bend at distances of a) 5, b) 50, and c) 95% of flow depth from bed.

The streamlines angles in various plans

In Figure 7, the averages of the horizontal angles of the streamlines in various cross sections have been compared at different flow depths in depth (at distances of 5, 50, and 95% of the flow depth from bed). The streamlines are highly diverted from the horizon at all three levels, but halfway through the bend, they have less diversion. As seen in the figure, the streamlines deviation at layer near water surface is higher than that at the other two layers. According to Figures 4, 5 and 6, this can be attributed to a shift from downstream to upstream lines because of formation of described clockwise vortices at analogous cross sections.

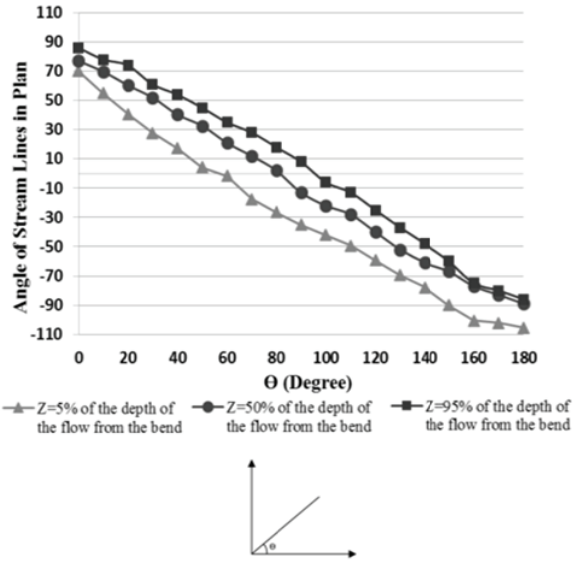

Figure 7. The averages of horizontal angles of the streamlines at different cross sections of the bend at distances of 5, 50, and 95% of the flow depth from bed.

From the beginning of the second half of bend, the streamlines reverse the orientation, and the highest amount of horizontal diversion of the streamlines is observed at the bend exit. Measurement of the averages of streamlines angles at different levels indicates that average difference of the angles between the streamlines at layers near the bed and those near surface is about 30 degrees in a clockwise direction, but the difference of the angles between the streamlines in the mid-depth of flow and those at layers near bed, as well as those at layers near surface, equals 9 degrees. The values mentioned for angle difference indicate the effect of sharp bend and the dominance of the longitudinal pressure gradient over the secondary flow in diverting streamlines at different layers of flow, especially at the lower layers.

Vectors and locus of the maximum velocity

In Figure 8, three examples of changes in flow velocity vectors as well as the locus of maximum velocity at levels of 5, 50 and 95% of the flow depth from bed are shown.

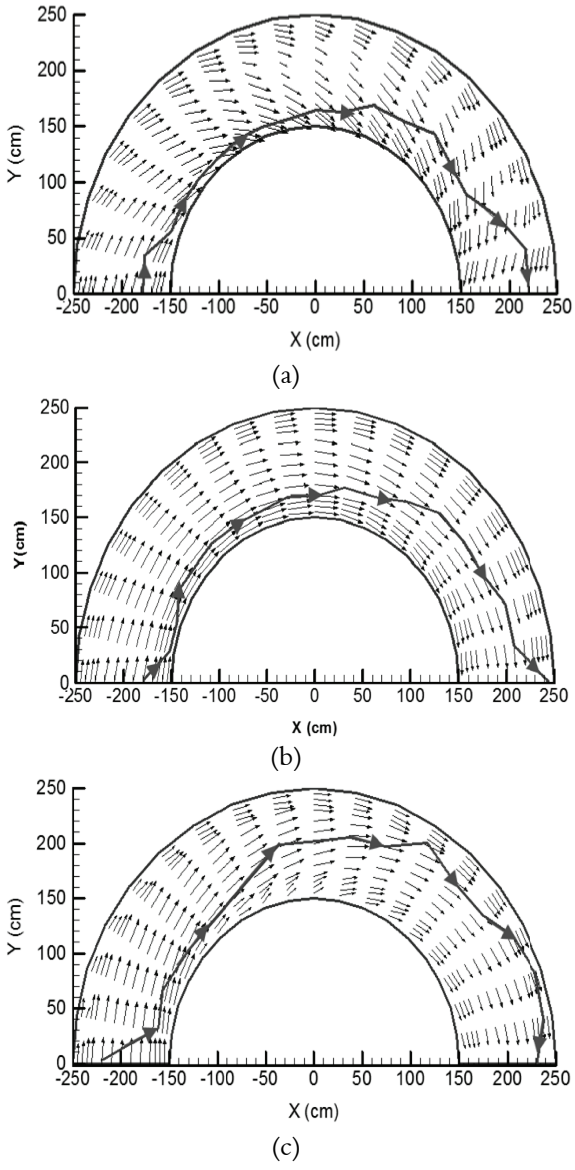

Figure 8. Vectors and locus of the maximum velocity in the plans of 180 degree sharp bend at distances of a) 5, b) 50, and c) 95 % of flow depth from bed.

First, at the level of 5% of flow depth from bed, the longitudinal flow is so strong all along the bend that it always dominates the secondary flow, and keeps the maximum velocity near the inner wall in all directions at the end of bend where, as shown in Figure 8a, the maximum velocity is again oriented towards outer wall due to the longitudinal pressure gradient at the bend exit. This continues in mid-depth of the flow (Figure 8b), but at the beginning of second half of bend, the maximum velocity occurs away from the inner wall, and at the end of the bend, it finally occurs near the outer wall. Near surface, the maximum velocity is most of the way oriented towards the outer bank, especially from the beginning of the second half of bend (Figure 8c).

These observations seem to be adequately in accordance with previous studies on two 180 degree bends conducted by Mockmore (1944) and those on a 180 degree bend with ratio of curvature radius to channel width equal to 1 done by Leschziner and Rodi (1979). As previously stated, the maximum velocity relocation occurs because, upon reaching the upper layers, the flow velocity and the centrifugal force increase. Therefore, the secondary flow grows stronger and the maximum velocities incline towards outer wall. By contrast, unlike the upper layer, the longitudinal pressure gradient at the lower layer always rules the secondary flow along the route and the maximum velocities of the flow remain close to the inner wall, except at the end of the route.

Conclusion

This paper investigated the streamlines and how they changed in a 180 degree sharp bend using measurement of 3D flow velocity by applying Vectrino in a laboratory flume. The results suggested that the size of the formed vortices increased from beginning to the middle of the bend in a way that two clockwise vortices were formed at the 90 degree cross section, at distances of 5 and 38% of the channel width from the inner bank. From the beginning of second half of bend to end, the core of the primary vortex moved away from the inner bank towards the mid-channel by 22%.

Nomenclature

PDMS: Polydimethylsiloxane; U: mean flow velocity; Uc: critical velocity; B: width of the channel; Z: water depth; x: longitudinal axis; y: lateral axis; and Θ: bend angle.

References

Abhari, M. N., Ghodsian, M., Vaghefi, M., & Panahpur, N. (2010). Experimental and numerical simulation of flow in a 90 degree bend. *Flow Measurement and Instrumentation, 21*(3), 292-298.

Baghalian, S., Bonakdari, H., Nazari, F., & Fazli, M. (2012). Closed-form solution for flow field in curved channels in comparison with experimental and numerical analyses and artificial neural network. *Engineering Applications of Computational Fluid Mechanics, 6*(4), 514-526.

Barbhuiya, A. K., & Talukdar, S. (2010). Scour and three dimensional turbulent flow fields measured by ADV at a 90 degree horizontal forced bend in a rectangular channel. *Flow Measurement and Instrumentation, 21*(3), 312-321.

Blanckaert, K., & Graf, W. H. (2001). Mean flow and turbulence in open-channel bend. *Journal of Hydraulic Engineering, 127*(10), 835-847.

Blanckaert, K., Kleinhans, M. G., McLelland, S. J., Uijttewaal, W. S. J., Murphy, B. J., Van de Kruijs, A., … Chen, Q. (2013). Flow separation at the inner (convex) and outer (concave) banks of constant□width and widening open channel bends. *Earth Surface Processes and Landforms, 38*(7), 696-716.

Bonakdari, H., Baghalian, S., Nazari, F., & Fazli, M. (2011). Numerical analysis and prediction of the velocity field in curved open channel using artificial neural network and genetic algorithm. *Engineering Applications of Computational Fluid Mechanics, 5*(3), 384-396.

Celik, A. O., Diplas, P., & Dancey, C. L. (2014, February). Instantaneous pressure measurements on a spherical grain under threshold flow conditions. *Journal of Fluid Mechanics, 741*, 60-97.

Chan, H. C., Zhang, Y., Leu, J. M., & Chen, Y. S. (2010). Numerical calculation of turbulent channel flow with porous ribs. *Journal of Mechanics, 26*(1), 15-28.

Constantinescu, G., Koken, M., & Zeng, J. (2011). The structure of turbulent flow in an open channel bend of strong curvature with deformed bed: Insight provided by detached eddy simulation. *Water Resources Research, 47*(5), 1-17.

Gholami, A., Akhtari, A. A., Minatour, Y., Bonakdari, H., & Javadi, A. A. (2014). Experimental and numerical study on velocity fields and water surface profile in a strongly-curved 90° open channel bend. *Engineering Applications of Computational Fluid Mechanics, 8*(3), 447-461.

Horvat, Z., Isic, M., & Spasojevic, M. (2015). Two dimensional river flow and sediment transport model. *Environmental Fluid Mechanics, 15*(3), 595-625.

Huang, C. Y., Li, C. A., Huang, B. H., & Liou, T. M. (2014). The study of temperature rise in a 90-degree sharp bend microchannel flow under constant wall temperature condition. *Journal of Mechanics, 30*(6), 661-666.

Huang, S. L., Jia, Y. F., Hsun-Chuan, C. H. A. N., & Sam, S. Y. (2009). Three-dimensional numerical modeling of secondary flows in a wide curved channel. *Journal of Hydrodynamics*, *Ser. B, 21*(6), 758-766.

Kra, E. Y., & Merkley, G. P. (2004). Mathematical modeling of open-channel velocity profiles for float method calibration. *Agricultural Water Management, 70*(3), 229-244.

Leschziner, M. A., & Rodi, W. (1979). Calculation of strongly curved open channel flow. *Journal of the Hydraulics Division, 105*(10), 1297-1314.

Mockmore, C. A. (1944). Flow around bends in stable channels. *Transactions of the American Society of Civil Engineers, 109*(1), 593-618.

Rozovskii, I. L. (1961). *Flow of water in bends of open channels*. Kiev, UA: Academy of Sciences of the Ukrainian SSR, Institute of Hydrology and Hydraulic Engineering.

Stoesser, T., Ruether, N., & Olsen, N. R. B. (2010). Calculation of primary and secondary flow and boundary shear stresses in a meandering channel. *Advances in Water Resources, 33*(2), 158-170.

Sui, J., Fang, D., & Karney, B. W. (2006). An experimental study into local scour in a channel caused by a 90 bend. *Canadian Journal of Civil Engineering, 33*(7), 902-911.

Termini, D. (2015, July). Momentum transport and bed shear stress distribution in a meandering bend: Experimental analysis in a laboratory flume. *Advances in Water Resources, 81*, 128-141.

Vaghefi, M., Akbari, M., & Fiouz, A. R. (2014). Experimental investigation on bed shear stress distribution in a 180 degree sharp bend by using Depth-Averaged method. *International Journal of Scientific Engineering and Technology, 3*(7), 962-965.

Vaghefi, M., Akbari, M., & Fiouz, A. R. (2015). Experimental investigation of the three-dimensional flow velocity components in a 180 degree sharp bend. *World Applied Programming, 5*(9), 125-131.

Van Balen, W., Uijttewaal, W. S. J., & Blanckaert, K. (2009, July). Large-eddy simulation of a mildly curved open-channel flow. *Journal of Fluid Mechanics, 630*, 413-442.

Wang, H., Zhou, G., & Shao, X. (2010). Numerical simulation of channel pattern changes Part I: Mathematical model. *International Journal of Sediment Research, 25*(4), 366-379.

Received on August 29, 2015.
Accepted on June 8, 2016.